Available online at www.sciencedirect.com

ScienceDirect

Procedia CIRP 75 (2018) 220–225

www.elsevier.com/locate/procedia

15th CIRP Conference on Computer Aided Tolerancing – CIRP CAT 2018

# Statistical Tolerance Analysis with T-Maps for Assemblies

Gaurav Ameta[a*1], Joseph K. Davidson[b] and Jami J. Shah[c]

[a] *Dakota Consulting Inc, Silver Spring, MD, USA*
[b] *Arizona State University, Tempe, AZ, USA, 85287*
[c] *The Ohio State University, Columbus, OH, USA, 43210*

* Corresponding author. Tel.: +0-000-000-0000 ; fax: +0-000-000-0000. *E-mail address:* gaurav.ameta@dakota-consulting.com

**Abstract**

The T-Map® (Tolerance-Map®) model for representing geometric variations of planar surfaces is extended to include probabilistic representations of variations of those surfaces. T-Maps are hypothetical volume of points, which can arise from tolerances on size, position, orientation, and form. The variations of a planar surface are decomposed into manufacturing and geometric bias. Statistical accumulation of variation in an assembly is computed using convolution of T-Maps. The dimension of interest is mapped to a surface *Sc* in the hypothetical Euclidean space. Probability distribution is then computed as weighted surface area of intersection of the surface *Sc* with the convolved accumulation T-Map.



*Keywords:* Statistical Tolerance Analysis, Assemblies, Convolution

## 1. Introduction and purpose

The modern method of specifying tolerances is through geometric dimensioning and tolerancing (GD&T or GPS), as specified in the ASME Y14.5M Standard [1] and/or ISO 1101 [2]. For automation of the tolerance analysis/ allocation, a math model representing the standard is required. Various mathematical models have been developed for automating the analysis and synthesis of geometric tolerances; detailed reviews of these models are available in [3–11].

The objective of this paper is to explore further an alternative model when using probability to assign/analyze tolerances to the parts in an assembly. The method is based on using Tolerance-Maps ([12–17]) to produce probability density functions (PDFs) to classify the geometric possibilities of a feature in its tolerance-zone. The initial work on this method appears in [18] and [16]. The effect of form on the PDFs for planar features on single part is presented in [19]. In these works, only the geometric variations of the feature are considered: we presume manufacturing bias to be uniformly distributed over all geometric possibilities. The specific objectives of this paper are to demonstrate statistical accumulation of variation in an assembly with form variation and orientation tolerance to the development of PDFs (size and parallelism) for the target feature of assembly, and to illustrate how weightings from non-uniform manufacturing bias (for position, orientation and form) may influence the PDF that results. Of course, the model is robust enough to include more specific biases of specific machines and processes for manufacturing, a modeling that is helpful for concurrent design.

[1]Contributed to this research while at Arizona State University.

## 2. Worst-Case Tolerance Analysis with T-Maps

A Tolerance-Map® (T-Map®) is a hypothetical Euclidean point-space, the size and shape of which reflects all variational possibilities for a target feature. It is the range of points resulting from a one-to-one mapping from all the variational possibilities of a feature, within its tolerance-zone, to the Euclidean point-space. These variations are determined by the various tolerances that are specified on the feature.

2212-8271 © 2018 The Authors. Published by Elsevier B.V.
Peer-review under responsibility of the Scientific Committee of the 15th CIRP Conference on Computer Aided Tolerancing - CIRP CAT 2018.
10.1016/j.procir.2018.02.021

*2.1 The basis-tetrahedron*

The T-Map® for any combination of tolerances on a feature is constructed from a basis-simplex in a space of dimension $n$, the value of $n$ corresponding to the freedom of movement of the feature within the tolerance-zone; it is described with areal coordinates. We choose to position the four basis-points $\sigma_1$, $\sigma_2$, $\sigma_3$ and $\sigma_4$ as shown in Figure 1. At the four basis-points we place four masses $\lambda_1$, $\lambda_2$, $\lambda_3$, and $\lambda_4$ that may be positive or negative. So long as $\lambda_1+\lambda_2+\lambda_3+\lambda_4 \neq 0$, the position of $\sigma$, the centroid of these masses, is uniquely determined by the linear combination

$$(\lambda_1+\lambda_2+\lambda_3+\lambda_4)\sigma = \lambda_1\sigma_1+\lambda_2\sigma_2+\lambda_3\sigma_3+\lambda_4\sigma_4 \quad (1)$$

and we can make $\sigma$ assume any position in the space of $\sigma_1..\sigma_4$ by varying $\lambda_1$, $\lambda_2$, $\lambda_3$, and $\lambda_4$. For example, for $\lambda_1..\lambda_4$ all positive, $\sigma$ identifies any point *inside* tetrahedron $\sigma_1\sigma_2\sigma_3\sigma_4$. Consequently, the four $\lambda_i$'s can be normalized by setting

$$\lambda_1+\lambda_2+\lambda_3+\lambda_4 = 1; \quad (2)$$

then they are *areal* coordinates and

$$\sigma = \lambda_1\sigma_1+\lambda_2\sigma_2+\lambda_3\sigma_3+\lambda_4\sigma_4 \,. \quad (3)$$

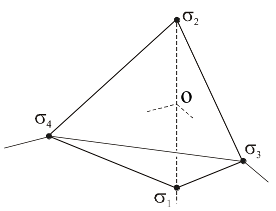

Figure 1. The basis tetrahedron with its basis points.

The shape of the basis-tetrahedron was chosen to simplify interpretation of T-Maps, particularly to decouple rotational and translational displacements in the tolerance-zone [12].

*2.2 The Tolerance-Map (T-Map®) for a Face with size tolerance*

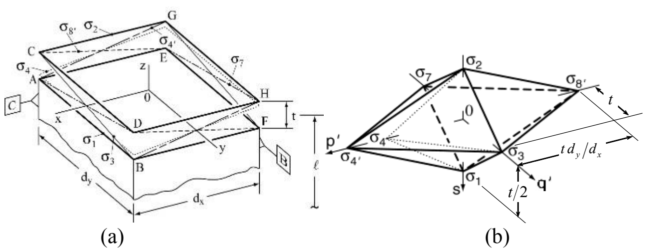

Figure 2. (a) The tolerance zone on size for a rectangular bar and a coordinate frame centered within it. (b) Corresponding T-Map for the tolerance zone in (a).

In Figure 2(a) is shown the end of a rectangular bar of cross-sectional dimensions $d_x \times d_y$ ( $d_x < d_y$ ). The length of the part shown is $\ell$ with an exaggerated tolerance $t$. According to the ASME Standard Y14.5 and/or ISO 1101, all points of the end-face must lie between the limiting planes $\sigma_1$ and $\sigma_2$, and within the rectangular limit of the face. The region defined by the limiting planes and the rectangular limit of the face is the tolerance-zone for the planar face.

A coordinate frame is located in the tolerance zone with its origin O at the geometrical center of the tolerance zone as shown in Figure 2(a). This coordinate frame has its axes parallel to the edges of the part. Presuming the face at first to be of perfect form, i.e. a rectangular *segment* of a plane, the possible placement of this face is against any one of a three-dimensional set of planes. Utilizing the parameters of each plane in the tolerance zone and the respective basis-tetrahedron, a mapping function is created between the planes in tolerance zone to points in the hypothetical space of the basis tetrahedron. Each of these planes in the tolerance zone is then mapped to a specific point in the T-Map®, as shown in Figure 2(b).

The construction of a T-Map ensures that each point inside it represents a single valid configuration of the feature within its tolerance-zone. The T-Map® for a planar face faithfully represents the 3-D variations permitted by the tolerance-zone: translation perpendicular to the plane and rotations about the $x$- and $y$- axes (Figure 2(a)). Measures along the $s$-axis of the T-Map® represent parallel variations of the plane negatively along the $z$-axis in the tolerance zone, while the $p'$- and $q'$- axes represent the orientational variations of the plane about the $y$- and $x$- axes, respectively. For further details about constructing the T-Map® in Figure 2(b), the reader is advised to refer to [20].

*2.3 Worst Case Tolerance Analysis*

Worst case tolerance analysis with T-Maps is conducted by following the steps listed below

1. Identify the features in the stack up from datum to target feature of the assembly.
2. Using the DRF's of each feature in the stack-up, create T-Maps for each.
3. Utilizing homogeneous transformation matrices to modify (conform) the individual T-Maps to represent the variations at the target feature of the assembly.
4. Accumulate the individual conformed T-Maps by utilizing Minkowski sum, thus creating an accumulation T-Map for the assembly.
5. Based on the target feature and dimension of interest, create a variable size T-Map (called functional T-Map) of the target feature.
6. Align the accumulation T-Map with the functional T-Map. Resize the functional T-Map until it circumscribes the accumulation T-Map. The dimensions of accumulation and functional T-Map leading to the points of contact between them reveals the stack up equation/value.

These steps have been demonstrated in detail with case studies in [12,15,20,21]. Next, we demonstrate the statistical model of tolerance zone for T-Map in order to conduct statistical tolerance analysis for assemblies.

## 3. Statistical Model of Tolerance-Zones And Dimensions of Interest From T-Maps

*3.1 Mathematical Definition of Probabilistic Representation of Variations*

Let $E_n$ be the $n$-dimensional Euclidean space in which the T-Map for a tolerance feature is defined. The parameters of the feature, controlled by the tolerances (as represented in the space $E_n$), are $e_1 \ldots e_n$. Let $A$ be the set of points representing a T-Map. Therefore, $A$ is an $n$-dimensional subset of the space $E_n$, i.e., $A \subseteq En$. $A$ can be chosen to depict an individual T-Map for part variations or an accumulation T-Map for assembly variations. The unit of the *content* of $A$ will be $(length)^n$. Let $B_c$ be the $n$-1 dimensional set of points defining the variations of the target feature that give a particular value $c$, for the dimension of the interest (such as clearance or height) i.e., $B_c \subseteq E_n$. The unit of the content of $B_c$ will be $(length)^{n-1}$. Let $Sc$ be the set of points inside the T-Map that define the variations of the target feature for a particular value of $c$, for the dimension of the interest (such as clearance) i.e., $S_c \subseteq A$, $S_c \subseteq B_c$. Therefore $Sc$ can be obtained as an intersection of $A$ and $B_c$ i.e., $S = A \cap B_c$. The unit of the content of $Sc$ will be $(length)^{n-1}$. The content of the set $Sc$ represents the frequency with which the value $c$ for the dimension of interest is obtained. Since $c$ is a continuous variable, the content of $Sc$ can be obtained by integrating over the set $S_c$. The probability density function can be obtained by evaluating the content of the set $S_c$. The probability density function is shown in equation (4), where $k$ is the reciprocal of the content of the set $A$ and $s_1 \ldots s_{n-1}$ are the parameters of the set $S_c$.

$$f(c) = k \int_{1} \ldots \int_{\substack{n-1 \\ S}} ds_{n-1} \ldots ds_1 \tag{4}$$

These are used to simplify the representation of the integration in equation (4). The unit of $k$ is $1/(length^n)$ and the unit of the content of $Sc$ is $(length)^{n-1}$. Therefore, the unit of $f(c)$ is $1/(length)$. When the probability density function is integrated between two parameters $c_1$ and $c_2$ having length units, the result is the probability that the value of $c$ will lie between $c_1$ and $c_2$;

$$P(c_1 \le c \le c_2) = \int_{c_1}^{c_2} f(c) dc = \int_{c_1}^{c_2} \left( k \int_{1} \ldots \int_{\substack{n-1 \\ S}} ds_{n-1} \ldots ds_1 \right) dc \tag{5}$$

For practical problems, such analytical integrations are complicated and cannot be automated. Therefore, numerical integration schemes will be used to demonstrate the application of the probability model proposed in this paper.

Manufacturing bias can be included by using a joint probability density function $g(e_1, e_2, \ldots, e_n)$ for the space $E_n$. This function $g(e_1, e_2, \ldots, e_n)$ can be used to influence the probability density function $f(c)$ as shown in equation (6).

$$f(c) = k' \int_{1} \ldots \int_{\substack{n-1 \\ S}} g(e_1, e_2, \ldots, e_n) ds_{n-1} \ldots ds_1 \tag{6}$$

where $k'$ is the probabilistic content of the set $A$. The probability that the value of $c$ will lie between $c_1$ and $c_2$ can be obtained as shown in equation (7).

$$P(c_1 \le c \le c_2) = \int_{c_1}^{c_2} f(c) dc = \int_{c_1}^{c_2} \left( k \int_{1} \ldots \int_{\substack{n-1 \\ S}} g(e_1, \ldots, e_n) ds_{n-1} \ldots ds_1 \right) dc \tag{7}$$

*3.2 Assemblies and Joint Probability Distributions*

The dimension of interest for Part 1 and Part 2 individually that are to be assembled to form an assembly will have a particular distribution of the variation of the feature within the tolerance zones and the corresponding T-Maps. When a worst-case tolerance analysis is being conducted, we combine the two T-Maps through the Minkowski sum; to find the convex hull, i.e. the boundary of the accumulation T-Map. For statistical analysis we are also interested in the probability distribution within the accumulation T-Map as a result of combining the probability density functions associated with the two operand T-Maps.

The Minkowski Sum is the convex hull (boundary points) of the vector addition of two convex hulls. Since in vector additions, each component (say $x$) is added to another component of the same type. For example, if $V_1(x_1, y_1, z_1)$ and $V_2(x_2, y_2, z_2)$, then $V_1 + V_2 = (x_1+x_2, y_1+y_2, z_1+z_2)$. We can obtain the probability density within the accumulation T-Map using the convolution. Convolution has been used to perform Minkowski Sums of concave polygons [22,23] and for combining multiple statistical distribution functions in the literature [24].

Since the shape of most accumulation T-Maps contains discontinuities of order $C^1$ (tangents) and/or $C^2$ (curvature), it is not feasible, in general, to analytically obtain the probability density function for the accumulation T-Map. Also T-Maps are multidimensional. Therefore, from a computational point of view, in this paper the development of the distribution of the sum of joint probability distributions will be demonstrated using the numerical "FFTW" package developed at MIT [25].

*3.3 Form and Orientation Tolerance*

Form variations are modeled as subset T-Maps within the size/position T-Maps. Each instance of form subset reduces the possible location and orientation variations. These subsets conform to the standard. Details of these subsets are provided in [12,19]. Equation (8) details this formulation with $\varphi$ representing form bias and the limits of $\varphi$ defining the limits of $S_1 \ldots S_n$ based on the concept of subsets.

$$f(c) = k'' \iint_{\varphi\, 1} \ldots \int_{\substack{n-1 \\ S}} \varphi \, ds_{n-1} \ldots ds_1 \, d\varphi \tag{8}$$

Orientation tolerances truncate the size/position T-Maps [12] based on the value and type of orientation tolerances. When parallelism is applied between two planar features, the lateral extent of a T-Map is truncated in all directions of the $p'q'$ plane (Figure 2(b)) by planes or cylindrical segments that are parallel to the $s$-axis. When perpendicularity is applied between two planar features, the T-Map is truncated along p' or q' axis depending on the relative orientation of the planar features. Form shape

*3.3 Properties of the Model*

3.3.1 Flexibility: The probability model developed in §3.1 can include any kind of manufacturing biases as shown in equation (6). These manufacturing biases can be included as a joint probability density function for the parameters of the space of the T-Map. Similarly, any kind of manufacturing biases for the distribution of the subset of form can be included using equation (8). Such manufacturing biases are dependent on various experimentally obtained factors, such as machine tool, material, machinist, environment etc.

3.3.2 Extensibility: The probability model of T-Maps presented in §3.1 is not specific to a feature, tolerance or dimension. Therefore, this probability model for T-Maps can easily be applied to any type of feature, tolerance and dimension as long as the T-Map model supports it. When applying the probability model of T-Map, the following characteristics need to be identified; Dimension of interest *c* and the Set *Sc*.

These characteristics will appear in examples in §4, §5 and §6. Since the developments for the accumulation T-Map and functional T-Map have already been discussed (§2.3), the identification of the Set *Sc* for each type of target feature and dimension of interest will be the most important step for applying the probability model of T-Map to different assembly examples.

## 4. Assembly of Two parts with height as dimension of interest

To demonstrate the application of the probability model, consider the assembly shown in Figure 3. Part 1 has a rectangular target face while part 2 has a circular target face. The assembly's dimension of interest is the maximum height from datum A.

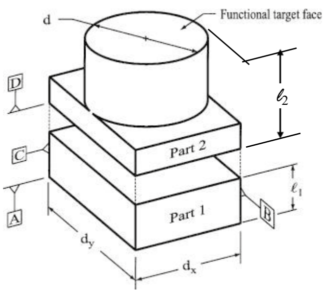


Figure 3. Assembly of two parts with dimensions $\ell_1$ and $\ell_2$.

### 4.1 Only Size Tolerance

When only size tolerances are considered ($t_1$ and $t_2$ on dimensions $\ell_1$ and $\ell_2$), the T-Map for part 1 is shown in Figure 2(b) while the T-Map for part 2 is a dicone with its axis along the *s*-axis. Manufacturing bias is considered uniform for this case and no form variations are considered. The T-Map for part 1 is conformed to the target circular face by scaling it along the dy-dimension with the ratio $d_x/d_y$. Then, convolution of the two T-Maps results in a convolved accumulation T-Map, as shown in Figure 4(a,1). Distinct colors in Figure 4(a,1) indicate change in density within the convolved accumulation T-Map by 25% due to convolution. The value of $t_1$ and $t_2$ for the case study is assumed to be 1.

The surface *Sc* can be identified from the target face as the top conical surface of the dicone. Surface area of intersection of the *Sc* with the convolved accumulation T-Map provides the frequency distribution of a particular height value (based on the location of *Sc*) of the assembly. This intersection surface for three different height values is shown in Figure 4(a,2). The resultant PDF is shown in Figure 5 with dashed gray lines.

### 4.2 With Form Variations

When form variations are considered within the tolerance-zone for size, multiple subset T-Maps for form are generated representing different amount of form variations. In this case, manufacturing bias and form variations are considered to be uniform across the entire size-zone. This implies that form variation of 0 is equally likely as form variation of $t_1/2$ or $t_1$. Individual T-Map densities (weights) are computed based on sum of weights from all subsets for form variations. For details please refer to [19]. Then, the weighted T-Maps for two parts with form variations are convolved resulting in the convolved accumulation T-Map depicted in Figure 4(b,1).

The surface *Sc* remains the same as in§ 4.1 but the intersections and the weights on intersection area change as depicted in Figure 4(b,2). The resulting PDF is shown in

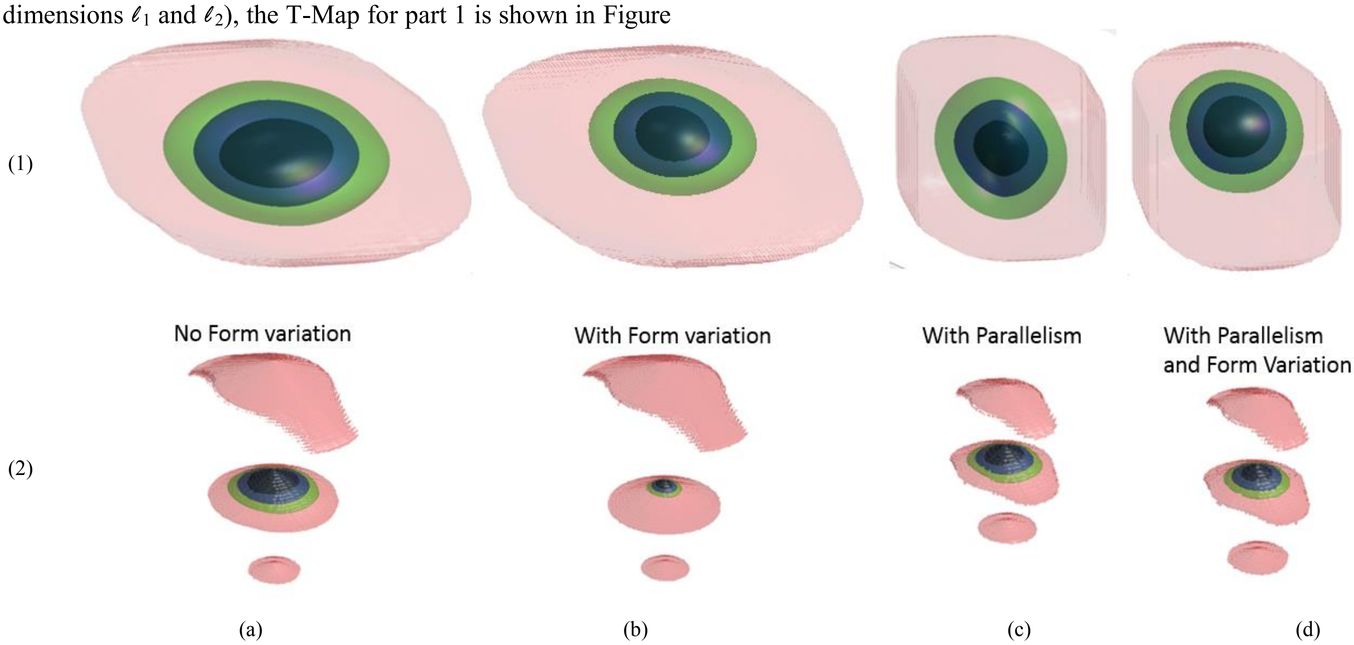


Figure 4:Convolved accumulation T-Map and intersection of *Sc* for different values of dimension of interest. Colors indicate relative weight values. Red - 0.1%, green -25%, blue-50% and black-75%. Row (1) displays different convolved accumulation T-Map while row (2) displays the corresponding intersection with surface *Sc* for particular values of dimension of interest. Each column represents four different cases in§ 4. (a) With size tolerance but not form variations (b) size tolerance and form variations (c) size and parallelism tolerance but no form variation and (d) size and parallelism tolerance with form variation.

Figure 5 with gray continuous line. As is evident, the impact of including form is to shift the mean towards larger heights.

*4.3 With Parallelism tolerance*

When parallelism tolerances for part 1 ($t_1/2$) and part 2 ($t_2/2$) with respect to datum A and D, respectively, are included, the corresponding T-Maps get truncated all around the T-Map edge in the *p'q'* plane. The resultant convolved T-Maps, without and with form variations, are shown in Figure 4(c,1) and Figure 4(d,1) respectively. The surface *Sc* remains the same as in§ 4.1 but the intersections and weights change as shown in Figure 4(c,2) and Figure 4(d,2). The resultant PDF without and with form variations are shown in Figure 5 with black dashed and continuous, lines respectively. Comparing back and gray lines, it is evident that the impact of parallelism tolerance is to shift the mean towards lower height while form variations push the mean towards higher height values. Furthermore, form variations also causes the distribution of the height to be narrower.

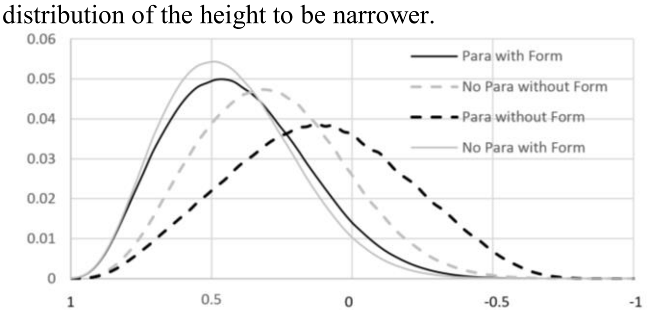


Figure 5: PDF for different cases shown in Figure 4. The horizontal axis represents variation from nominal height value ($\ell_1 + \ell_2$) of the assembly. The vertical axis represents the relative frequency distribution.

*4.4 With Manufacturing Bias*

In this model manufacturing bias can be included as a distribution, as sets (with probability as weights), or combination of both. A truncated gaussian distribution as manufacturing bias for PDF of single part is already demonstrated in [19]. Here we will demonstrate manufacturing bias for (a) form variation as a set and (b) height variation below nominal as a function. Form variation below value t/2 will have zero likelihood while form variation from t/2 to t will be equally likely (weight 1.0). Similarly, height variation above nominal will be equally likely (weight 1.0) while height variation below nominal will have weight = $1+(10\text{X}|h_0\text{-}h_i|)^3$, where $h_0$ is nominal height while $h_i$ is height

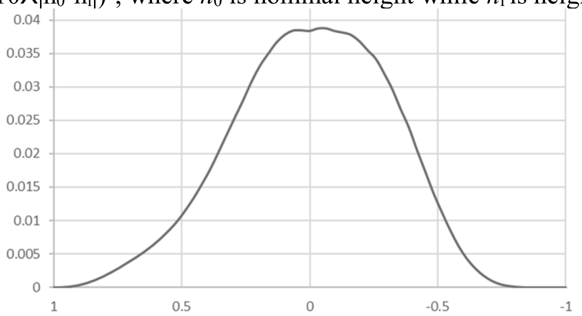


Figure 6: PDF for manufacturing bias in form and height of the planar feature in a two-part assembly shown in Figure 3.

value of a point within the T-Map of individual part. The resulting PDF following the analysis is shown in Figure 6. Compared to the PDFs of Figure 5, this particular manufacturing bias has shifted the mean of PDF towards the nominal value.

## 5. Assembly of Two parts with evaluated parallelism zone size as dimension of interest

In the assembly of Figure 3, if the functional dimension of interest was the size of evaluated parallelism zone of the target feature, then the shape of surface *Sc* will be changed. It will be a cylinder of varying radius based on the size of evaluated parallelism zone. All other steps for creating convoluted accumulation T-Maps will be the same as in §4. An intersection, and the weighted surface area of intersection, needs to be recomputed based on new Sc. Two sets of intersection surfaces are shown for new *Sc* in Figure 8, without and with parallelism tolerance specified. Four resultant PDFs are shown in Figure 7. When a parallelism tolerance is not specified, the worst case size of evaluated parallelism zone is $t_1$+$t_2$ (=2). When a parallelism tolerance t/2 is specified, the worst case size of evaluated parallelism zone is 0.5 ($t_1$+$t_2$)=1. As in Figure 5, form variation causes the mean of PDF to shift towards the left. Parallelism tolerance specification also causes the mean of PDF to shift left, because of change in the worst case value.

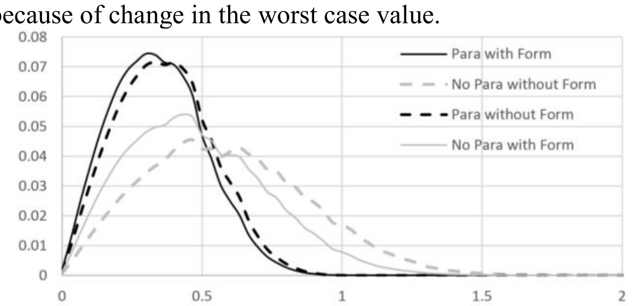


Figure 7: PDF for different cases from Figure 4 with size of evaluated parallelism zone being the dimension of interest.

## 6. Linearly Stacked Assembly of multiple parts

To understand the impact of an assembly of multiple parts, (i.e. convolution) we consider an assembly of *n* similar parts (rectangular) with same lateral dimensions stacked one on top of another. The tolerances of *n* parts add to 0.7. Therefore, the size tolerance on each part is 0.7/*n*. Now we vary n from 1 to seven and follow the statistical model discussed in §4 to understand the impact of number of parts in an assembly by developing PDFs. For the development of these PDFs', form variation is ignored. These PDFs are shown in Figure 9. As the value of *n* increases, the mean shifts towards the nominal value and the variance reduces.

## 7. Conclusion

This paper demonstrated the flexibility and extensibility of the probability model of T-Maps. To represent assembly of parts statistically, convolution of weighted T-Maps, resulting in convoluted accumulation T-Map, was proposed followed by intersection with a surface *Sc*. Surface *Sc* is obtained by


Figure 8: Different instances of intersection of surface *Sc* for the dimension of interest being the size of evaluated parallelism zone. (a) with no parallelism tolerance specified and (b) with parallelism tolerance (t/2) specified.

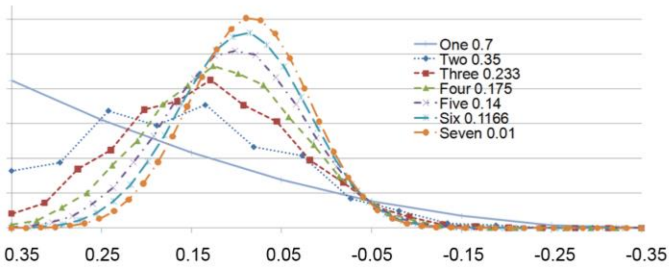


Figure 9: Effect of number of parts in stack up on the PDF of height of the assembly.

identifying the dimension of interest for the assembly and its mapping in the T-Map space. The PDF of the dimension of interest was developed from the weighted area of the intersection of *Sc* and the convoluted accumulation T-Map for the assembly. The effect of form variations, orientation tolerances, manufacturing biases (on form and height variations) and two different dimensions of interest were demonstrated on the resultant PDF. The PDF can be utilized for statistical tolerance allocation thereby loosening tolerances (reducing costs) while scrapping only a small percentage of assemblies.

## References:

[1] ASME Y14.5-2009: Dimensioning and Tolerancing, ASME, New York, NY.
[2] ISO 1101:2017 - Geometrical Product Specifications (GPS) -- Geometrical Tolerancing -- Tolerances of Form, Orientation, Location and Run-Out, ISO.
[3] Shen Z, Ameta G, Shah JJ, Davidson JK. A Comparative Study Of Tolerance Analysis Methods. J Comput Inf Sci Eng 2005;5:247.
[4] Shah JJ, Ameta G, Shen Z, Davidson J, Navigating the Tolerance Analysis Maze. Comp Aid Des App 2007;4.
[5] Ameta G, Samper S, Giordano M. Comparison of Spatial Math Models for Tolerance Analysis: Tolerance-Maps, Deviation Domain, and TTRS. J comp inf sci eng 2011;11.
[6] Mansuy M, Giordano M, Davidson JK. Comparison of Two Similar Mathematical Models for Tolerance Analysis: T-Map and Deviation Domain. J Mech Des 2013;135:101008.
[7] Hong YS, Chang TC. A Comprehensive Review of Tolerancing Research. Int JProd Res 2002;40:2425–59.
[8] Marziale M, Polini W. A Review of Two Models for Tolerance Analysis of an Assembly: Vector Loop and Matrix. Int J Ad Manuf Technol 2009;43:1106–23.
[9] Polini W. Taxonomy of Models for Tolerance Analysis in Assembling. Int J Prod Res 2012;50:2014–29.
[10] Marziale M, Polini W. Review of Variational Models for Tolerance Analysis of an Assembly. Proc Inst Mech Eng B 2011;225:305–18.
[11] Marziale M, Polini W, A Review of Two Models for Tolerance Analysis of an Assembly: Jacobian and Torsor. Int J Comput Integr Manuf 2011;24:74–86.
[12] Davidson JK, Mujezinović A, Shah JJ. A New Mathematical Model for Geometric Tolerances as Applied to Round Faces. J mech des 2002;124:609–22.
[13] Davidson JK, Shah JJ. Geometric Tolerances: A New Application for Line Geometry and Screws. Proc Inst Mech Eng C 2002;216:95–103.
[14] Ameta G, Davidson JK, Shah JJ. The Effects of Different Specifications on the Tolerance-Maps for an Angled Face. In: International Design Engineering and Technical Conference, ASME.
[15] Ameta G, Davidson JK, Shah, JJ. Tolerance-Maps Applied to a Point-Line Cluster of Features. J Mech Des 2007;129:782.
[16] Ameta G. Statistical Tolerance Analysis and Allocation for Assemblies Using Tolerance-Maps. Ph.D. Thesis, Arizona State University 2006.
[17] Rao SS, Haghighi P, Shah JJ, Davidson JK. Library of T-Maps for Dimensional and Geometric Tolerances. In: ASME 2014 International Design Engineering Technical Conferences and Computers and Information in Engineering Conference, American Society of Mechanical Engineers 2014, p. V004T06A019–V004T06A019.
[18] Ameta G, Davidson JK, Shah JJ. Allocating Tolerances Statistically with Tolerance-Maps and Beta Distributions: The Target a Planar Face. In: Proceedings of the ASME IDETC, Long Beach, CA, USA 2005, p. 28.
[19] Ameta G, Davidson JK, Shah JJ. Influence of Form on Tolerance-Map-Generated Frequency Distributions for 1D Clearance in Design. Precis Eng 2010;34:22–27.
[20] Mujezinović A, Davidson JK, Shah JJ. A New Mathematical Model for Geometric Tolerances as Applied to Polygonal Faces. J Mech Des 2004;126:504.
[21] Jian AD, Ameta G, Davidson JK, Shah JJ. Tolerance Analysis and Allocation Using Tolerance-Maps for a Power Saw Assembly. In: Proceedings of the 9th CIRP Seminar on Computer Aided Tolerancing, on CD-ROM, Springer 2005.
[22] Hartquist EE, Menon JP, Suresh K, Voelcker HB, Zagajac J. A Computing Strategy for Applications Involving Offsets, Sweeps, and Minkowski Operations. Comput Aided Des 1999;31:175–83.
[23] Guibas LJ, Seidel R. Computing Convolutions by Reciprocal Search. Discrete Comput Geom 1998;2:175–93.
[24] Sheldon R, and others. A First Course in Probability. Pearson Education India 2002.
[25] Frigo M, Johnson SG. FFTW: An Adaptive Software Architecture for the FFT. In: Proceedings of the 1998 IEEE International Conference On Acoustics, Speech and Signal Processing, IEEE 1998, pp. 1381–4.